

Modeling of type-II quantum dot intermediate band solar cells accounting for thermal and optical intersubband transitions

Original

Modeling of type-II quantum dot intermediate band solar cells accounting for thermal and optical intersubband transitions / Khalili, A.; Cappelluti, F.. - ELETTRONICO. - 2018-:(2018), pp. 139-140. (18th International Conference on Numerical Simulation of Optoelectronic Devices, NUSOD 2018 chn 2018) [10.1109/NUSOD.2018.8570264].

Availability:

This version is available at: 11583/2738316 since: 2019-06-30T15:54:26Z

Publisher:

IEEE Computer Society

Published

DOI:10.1109/NUSOD.2018.8570264

Terms of use:

This article is made available under terms and conditions as specified in the corresponding bibliographic description in the repository

Publisher copyright

IEEE postprint/Author's Accepted Manuscript

©2018 IEEE. Personal use of this material is permitted. Permission from IEEE must be obtained for all other uses, in any current or future media, including reprinting/republishing this material for advertising or promotional purposes, creating new collecting works, for resale or lists, or reuse of any copyrighted component of this work in other works.

(Article begins on next page)

Modeling of type-II quantum dot intermediate band solar cells accounting for thermal and optical intersubband transitions

Arastoo Khalili, Federica Cappelluti

Department of Electronics and Telecommunications, Politecnico di Torino, Torino, Italy
arastoo.khalili@polito.it

Abstract—Novel solar cell concepts relying on the use of nanostructures requires *ad hoc* device modeling tools able to cope with carrier transport and charge transfer mechanisms involving the host bulk material and the quantum confined states. In this work we apply such approach to study the implication of intersubband competitive processes in type-II GaSb/GaAs quantum dots on their application to intermediate band solar cells.

Quantum dots have been investigated since several years for demonstrating intermediate band solar cells (IBSC) [1]. Intraband transitions enabled by the 3D confinement allow the so-called two photon absorption (TPA) process producing an extra photocurrent while maintaining a high photovoltage, resulting in a theoretical efficiency well above that one of single junction cells. Type-I InAs/GaAs QDs have been very extensively studied and the IBSC operating principles proven. However, temperature-assisted intraband escape processes compete with the second photon absorption to such an extent that observation of TPA generally requires cryogenic temperatures, and the reported QD cells usually work in a thermally-limited operating regime. On the other hand, models of IBSCs [2] usually neglect thermally activated transitions, and thus have limited application to the analysis and design of practical devices. To fill this gap, we have recently proposed a drift-diffusion based model of QD solar cells which includes a proper treatment of quantum carrier capture and escape [3] and proven its ability to explain inherent limitations and experimental results of InAs/GaAs QD solar cells [4], [5].

In this work, we apply the model to study IBSCs based on GaSb/GaAs QDs (see Fig.1), whose intersubband dynamics are more promising than those of the InAs/GaAs QDs in view of attaining the IB operating regime. In fact, GaSb/GaAs QDs are characterized by high energy confinement in the valence band (VB) (between 0.4 and 0.49 eV [6]–[9]) and by staggered band alignment (type-II, see Fig.1(b)). The reduced overlap between electron and hole wavefunctions causes a carrier radiative lifetime on the order of 10 ns [10], [11], about ten times larger than that one of InAs/GaAs QDs.

The impact of the GaSb/GaAs QDs on the electrical performance of IBSCs is studied based on the simple $p-i-n$ structure shown in Fig.1(a), which includes 5 QD layers within a 100 nm thick intrinsic region. The assumed GaSb/GaAs QD parameters are summarized in Table I.

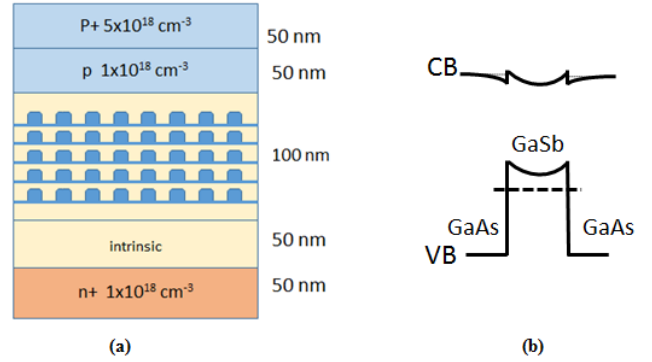


Fig. 1. (a) The solar cell structure used in the simulation. (b) GaSb/GaAs quantum-dot with staggered band alignment.

TABLE I
TYPE-II GASB/GAAS QD PARAMETERS

QD in-plane density [cm^{-2}]	1×10^{11}
$\Delta E_{\text{VB-GS}}$ [eV]	0.25-0.40
$\tau_{\text{CAP,VB-GS}}^h$ [ps]	5 [12]
τ_r^{GS} [ns]	10
GS degeneracy	6
$\alpha_{\text{IB} \rightarrow \text{CB}}$ [cm^{-1}]	10^3
$\alpha_{\text{IB} \rightarrow \text{VB}}$ [cm^{-1}]	10^4

The device is analyzed by a 1D drift-diffusion model completed by a rate equation that links the 3D bulk carrier densities to the QD confined carrier densities in each dot layer [3]. according to the schematic model shown in Fig.2, which describes the interband radiative transitions ($G_{\text{ph}}^{\text{BB}}$, and $R_{\text{QD}}^{\text{rad}}$) and the intersubband net thermal ($R_{\text{ESC}}^{\text{Thermal}}$) and radiative (G_{ph}^{2nd}) escape processes. QD layers are assumed uncoupled to the large interdot layer thickness.

Fig.3 shows the calculated net thermal and TPA escape rates for different QD confinement energy, highlighting the suppression of thermal emission as the confinement energy increases and the onset of dominant optical emission at high concentration in agreement with the results in [13]. The thermally-limited and IB operating regime for the cells with shallow and deep confinement QDs, respectively, is shown

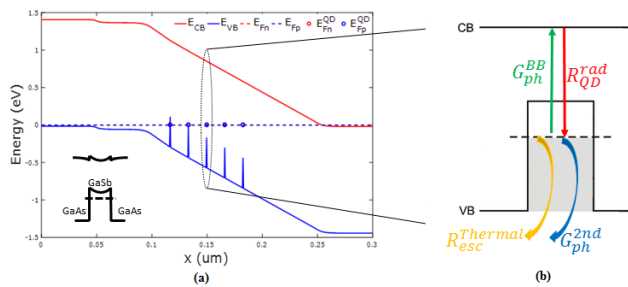


Fig. 2. (a) Thermal equilibrium band diagram of the cell under study. (b) QD model with relevant interband and intersubband transitions.

in Fig.4. The thermally limited regime is characterized by a logarithmic dependence of V_{oc} on the sun concentration (XSUN) - according to the diode equation in radiative limit -, whereas the IB operating regime is characterized by a stronger dependence of V_{oc} on concentration, confirming the theoretical predictions in [2] which were derived neglecting thermally activated escape. In fact, in the IB regime a larger carrier injection is needed to compensate for the increase of TPA-driven escape as the concentration increases.

Going further, and exploring the use of QD doping and the possibility to enhance the TPA by light-trapping approaches [14], simulations show that cells with deeply confined QDs the onset of truly IB regime can be pursued at markedly lower concentrations, on the order of tens of sun.

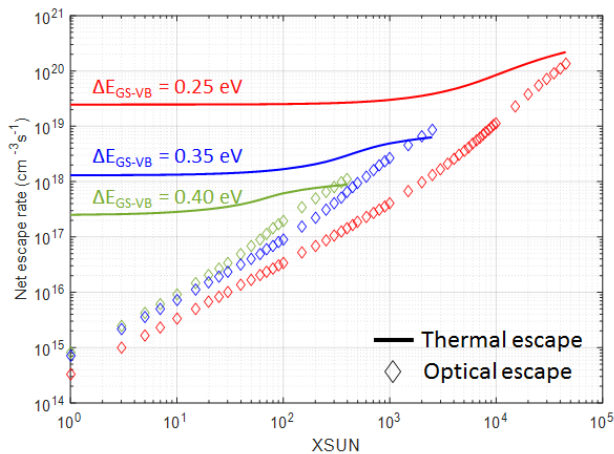


Fig. 3. Thermal and optical emission rate of charges from the GS to the VB continuum, considering confinement levels of 0.25, 0.3 and 0.4 eV within the VB.

REFERENCES

- [1] A. Luque and A. Martí, "Increasing the efficiency of ideal solar cells by photon induced transitions at intermediate levels," *Physical Review Letters*, vol. 78, no. 26, p. 5014, 1997.
- [2] K. Yoshida, Y. Okada, and N. Sano, "Device simulation of intermediate band solar cells: Effects of doping and concentration," *Journal of applied physics*, vol. 112, no. 8, p. 084510, 2012.

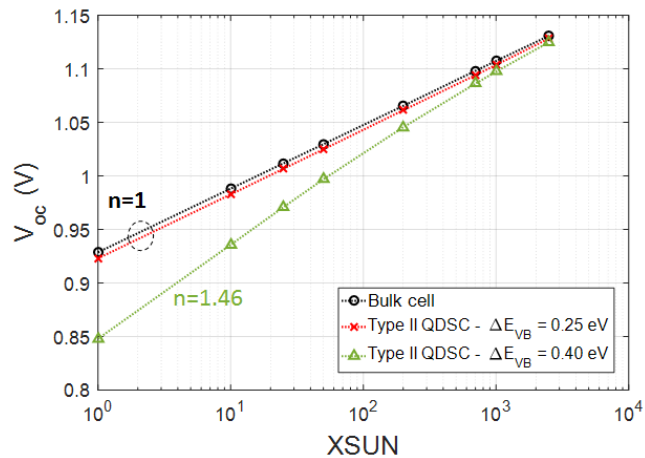


Fig. 4. Evolution of open circuit voltage with respect to sun concentration for QDSC with Type-II band alignment with shallow (0.25 eV) and deep (0.4 eV) confinement within the VB. The open circuit voltage behavior of the bulk cell is also shown.

- [3] M. Gioannini, A. P. Cedola, N. Di Santo, F. Bertazzi, and F. Cappelluti, "Simulation of quantum dot solar cells including carrier intersubband dynamics and transport," *IEEE Journal of Photovoltaics*, vol. 3, no. 4, pp. 1271–1278, 2013.
- [4] F. Cappelluti, M. Gioannini, and A. Khalili, "Impact of doping on inas/gaas quantum-dot solar cells: a numerical study on photovoltaic and photoluminescence behavior," *Solar Energy Materials and Solar Cells*, vol. 157, pp. 209–220, 2016.
- [5] A. Cédola, D. Kim, A. Tibaldi, M. Tang, A. Khalili, J. Wu, H. Liu, and F. Cappelluti, "Physics-based modeling and experimental study of si-doped inas/gaas quantum dot solar cells," *International Journal of Photoenergy*, vol. 2018, 2018.
- [6] M. Geller, C. Kapteyn, L. Müller-Kirsch, R. Heitz, and D. Bimberg, "450 meV hole localization in gasb/gaas quantum dots," *Applied Physics Letters*, vol. 82, no. 16, pp. 2706–2708, 2003.
- [7] M. C. Wagoner, P. J. Carrington, J. R. Botha, and A. Krier, "Photocapacitance study of type-ii gasb/gaas quantum ring solar cells," *Journal of Applied Physics*, vol. 115, no. 1, p. 014302, 2014.
- [8] I. Ramiro, E. Antolín, J. Hwang, A. Teran, A. J. Martín, P. G. Linares, J. Millunchick, J. Phillips, A. Martí, and A. Luque, "Three-bandgap absolute quantum efficiency in gasb/gaas quantum dot intermediate band solar cells," *IEEE Journal of Photovoltaics*, vol. 7, no. 2, pp. 508–512, 2017.
- [9] M. Wagoner, P. Carrington, J. Botha, and A. Krier, "Evaluation of the two-photon absorption characteristics of gasb/gaas quantum rings," *Journal of Applied Physics*, vol. 116, no. 4, p. 044304, 2014.
- [10] B. Liang, A. Lin, N. Pavarelli, C. Reyner, J. Tatebayashi, K. Nunna, J. He, T. J. Ochalski, G. Huyet, and D. L. Huffaker, "Gasb/gaas type-ii quantum dots grown by droplet epitaxy," *Nanotechnology*, vol. 20, no. 45, p. 455604, 2009.
- [11] C.-K. Sun, G. Wang, J. Bowers, B. Brar, H.-R. Blank, H. Kroemer, and M. Pilkuhn, "Optical investigations of the dynamic behavior of gasb/gaas quantum dots," *Applied physics letters*, vol. 68, no. 11, pp. 1543–1545, 1996.
- [12] K. Komolibus, T. Piwonski, C. Reyner, B. Liang, G. Huyet, D. Huffaker, E. Viktorov, and J. Houlihan, "Absorption dynamics of type-ii gasb/gaas quantum dots," *Optical Materials Express*, vol. 7, no. 4, pp. 1424–1430, 2017.
- [13] J. Hwang, A. J. Martin, J. M. Millunchick, and J. D. Phillips, "Thermal emission in type-ii gasb/gaas quantum dots and prospects for intermediate band solar energy conversion," *Journal of Applied Physics*, vol. 111, no. 7, p. 074514, 2012.
- [14] F. Cappelluti, M. Gioannini, G. Ghione, and A. Khalili, "Numerical study of thin-film quantum-dot solar cells combining selective doping and light-trapping approaches," in *Photovoltaic Specialists Conference (PVSC), 2016 IEEE 43rd*. IEEE, 2016, pp. 1282–1286.